

Automated Classification of Power Quality Disturbances using SVM and RBF Networks

P. Janik and T. Lobos

Abstract The authors propose a new method of power quality classification using SVM (Support Vector Machine) neural networks. Classifier based on RBF networks (Radial Basis Function) was in parallel applied to enable proper performance comparison. Both, RBF and SVM networks are introduced and considered an appropriate tool for classification problems. Space phasor is used for feature extraction from three-phase signals, to build distinguished patterns for classifiers. In order to create training and testing vectors different disturbance classes were simulated (e.g. sags, voltage fluctuations, transients) in Matlab. Finally, the investigation results of the novel approach are shown and interpreted.

Index Terms—Power Quality, Disturbance Classification, Neural Networks, Space Phasor, Support Vector Machines

I. INTRODUCTION

THE growing interest in power quality (PQ) issues should be viewed in a context of wide developments in power delivery engineering. Increased importance of PQ problems in industry and scientific community has many reasons [1], [2], [3]:

- the deregulation of the electricity market has caused growing need for standardization and performance criteria,
- electronic and power electronic equipment has become more sensitive to voltage disturbances than its counterparts in the past,
- modern power electronic equipment as well as other non-linear devices are not only sensitive to voltage disturbances but also cause disturbances for other customers.

Not only customers, but also internal phenomena in the supply system, can lead to PQ deterioration.

The ideal voltage curve in a three-phase electrical power network can be defined as follows: sinusoidal waveform, constant frequency according to the grid frequency, equal amplitudes in each phase according to the voltage level, defined phase-sequence with an angle of 120° between them. Every phenomenon, affecting those parameters, will be seen as decrease in voltage quality.

Automated monitoring methods are necessary for efficient processing of a large number of incidents especially in the case of wide area monitoring. Proposed method makes analysis of large data sets feasible. To apply this method in real time, automatic detection of the begin of incidents is necessary. As soon as a disturbance has been detected, the samples of voltages are collected and taken into the processing.

This paper proposes a new method for power quality classification using SVM (Support Vector Machines) neural networks. For comparison, a classifier based on the RBF networks was also investigated. The RBF and SVM networks are introduced and considered as an appropriate tool for classification problems. Additionally, main features of their architectures are shortly introduced.

For efficient feature extraction, three-phase voltage signals were transformed into space phasors to present distinctive patterns for the classifier. Applying the complex phasors enables reduction in computational effort.

Firstly, signals were simulated using parametric equations. Secondly, model of a power system built in Matlab was used for signals generation. Parameters variation helped to evaluate classification rate under different conditions. Finally, classification results are presented and discussed.

II. SUPPORT VECTOR MACHINE

Artificial neural networks (NN) with classical learning algorithms (minimizing nonlinear error function) show some important disadvantages [4], [5]. Firstly, the error function to be minimized is multi-modal with many local minima, where the learning process can get stuck. Secondly, the learning algorithm is not able to control the complexity of the architecture of NN, therefore the chosen architecture determines the generalization abilities.

In recent years, a new approach to construct and train neural networks was developed, which is free of such disadvantages. New networks are called Support Vector Machine (SVM) [6].

SVM implements a special training algorithm maximizing the separating margin between two classes, given by a set of p data pairs (input vector, class)

$$(x, d_i) \quad (1)$$

for $i=1,2,3\dots p$

SVM is unidirectional, has two layers and can implement different activation functions: linear, polynomial, radial or sigmoid.

For linear separable training pairs of two classes (1) the

This work was supported in part by Polish State Committee for Scientific Research under Grant 3T10A 00527.

P. Janik and T. Lobos are with Department of Electrical Engineering, Wrocław University of Technology, Wyb. Wyspińskiego 27, 50-370 Wrocław, Poland (e-mail:tadeusz.lobos@pwr.wroc.pl, przemyslaw.janik@pwr.wroc.pl)

separating hyperplane $g(x)$ is given by

$$g(x) = w^T x + b = 0 \quad (2)$$

where, w are weights, and b biases.

Hyperplane (2) is considered optimal when the separating margin between two classes is maximal, and this is achieved by computing (solving the primal problem)

$$\min_w \frac{1}{2} w^T w \quad (3)$$

and considering

$$d_i(w^T x_i + b) \geq 1 \quad (4)$$

This problem leads to minimization of the Lagrange function.

$$J(w, b, \alpha) = \frac{1}{2} w^T w - \sum_{i=1}^p \alpha_i [d_i(w^T x_i + b) - 1] \quad (5)$$

where α is non-zero Lagrange coefficient.

The equations (3) and (4) have different forms, if two classes are not linearly distributable. New objective function ϕ is given by

$$\phi(w, \xi) = \frac{1}{2} w^T w + C \sum_{i=1}^p \xi_i, \quad \xi_i > 0 \quad (6)$$

$$d_i(w^T x_i + b) \geq 1 - \xi_i \quad (7)$$

where ξ is so called fulfilling variable, C upper bound for α .

In this case, the SVM maps the input vectors x into a high dimensional space through some nonlinear mapping (ϕ function), where an optimal hyperplane is constructed [7],[8]. Schematic structure of the SVM network is shown in Fig. 1, where ϕ are activating functions.

Good classification properties of SVM have been shown in [6], [8].

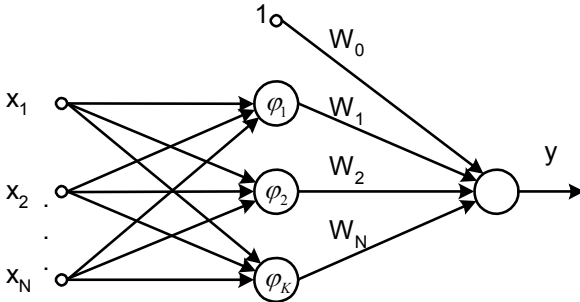


Fig. 1. Simplified Structure of Support Vector Machine Network

III. RADIAL BASIS FUNCTION NETWORKS

Radial Basis Function Networks RBF can be used as universal function approximations. They consist of a network with a single hidden layer and a structure similar to back propagation networks [9]. Investigation results presented in [10], [11], [12] confirm the advantages the RBF neural networks over the others solutions for classification tasks. Each hidden layer unit has a centroid c_i and smoothing factor σ_i . These neurons compute the distance between the input x_i

and the centroid c_i rather than the vector product of the weights and inputs. The outputs are nonlinear, radial symmetrical functions of the distance [9]. Thus, the output is the strongest when x_i is the closest to the value c_i . RBF networks apply real mapping functions f_m which has the general form

$$f_m(x) = \sum_{i=1}^M w_i K[(x_i - c_i)/\sigma_i] \quad (8)$$

The function K is a radial symmetric kernel function computed by M kernel units. Gaussian exponential function is commonly used in RBF networks

$$f(x) = \beta \exp\left(-\sum_i [(x_i - c_i)/\sigma_i]^2\right) \quad (9)$$

The centroid c_i , constants β and σ_i have to be chosen accordingly to training data set.

General Gaussian activation functions are superior to sigmoid functions [13] in estimating of a broad class of functions. The basic structure of a RBF network is similar to the SVM network (Fig.1), but instead of the activating function ϕ the exponential function (9) is applied.

IV. SPACE PHASOR

In order to construct sufficiently distinctive patterns for the SVM classifier, the idea of the space phasor was applied [14]. The most severe and dangerous sags occur during short circuits in distribution middle voltage networks. The neutral in such networks is in most cases isolated, earthed through a reactor or earthed through a resistor. The zero-sequence current component in case of a single-phase to earth fault in such networks reaches insignificant values. That is why we investigated only sags caused by two-phase and three-phase short circuits. Applying the complex space phasor enables to reduce the computational effort. Instead of three-phase real-valued signals we have to process one complex signal.

Construction of a space phasor requires three-phase signal. Complex space phasor \mathbf{f} is given by

$$\begin{bmatrix} f_1 \\ f_2 \end{bmatrix} = \sqrt{\frac{2}{3}} \begin{bmatrix} 1 & -\frac{1}{2} & -\frac{1}{2} \\ 0 & \frac{\sqrt{3}}{2} & -\frac{\sqrt{3}}{2} \end{bmatrix} \begin{bmatrix} f_a \\ f_b \\ f_c \end{bmatrix} \quad (10)$$

and

$$\mathbf{f} = \frac{f_1 + jf_2}{\sqrt{2}} \quad (11)$$

The space phasor rotates with angular velocity of the main component ω . In addition to the positive-sequence component, it describes an existing negative-sequence component as well as harmonic and non-harmonic components.

A further step in reducing the amount of input data for the classifier and obtaining more distinctive pattern could be undertaken. It can be achieved by stopping the rotating space vector by multiplication with the operator $e^{-j\omega t}$.

V. DETECTION OF DISTURBANCES

A fast and efficient means of analyzing voltage waveforms during power systems disturbances are the wavelet transforms. For detection of appearances of sags a multi-resolution analysis tree has been applied [15]. Every one of the wavelet transform sub-bands is reconstructed separately from each other, so we get $k+1$ separated components of a signal $x[n]$. The analysis tree is shown in Fig. 2 for the case when $k=2$. The outputs of the tree are detail signals. The *approximations* (A) are the high-scale, low frequency components of the signal. The *details* (D) are the low-scale, high frequency components. We applied *multires* function (built in MATLAB), which calculates the approximation to the 2^k scale and the difference or detail signals from the 2^1 to the 2^k scale for a given input signal $x[n]$. It uses the analysis filters h (low pass) and g (high pass) and the synthesis filters rh (low pass) and rg (high pass). We used the sixth order Daubechies filter (Fig. 3).

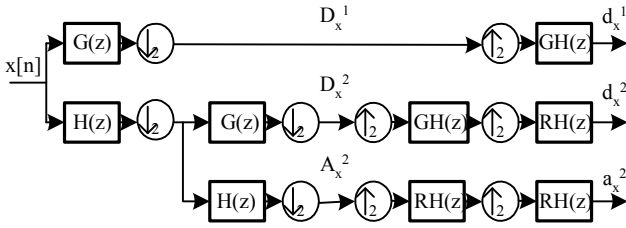


Fig. 2. Analysis-Synthesis tree for the MATLAB *multires* function.

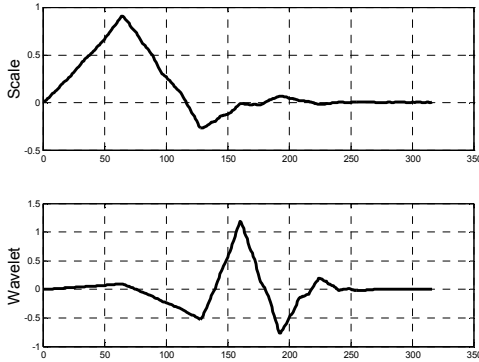


Fig. 3. Scaling and wavelet function of sixth order Daubechies filter

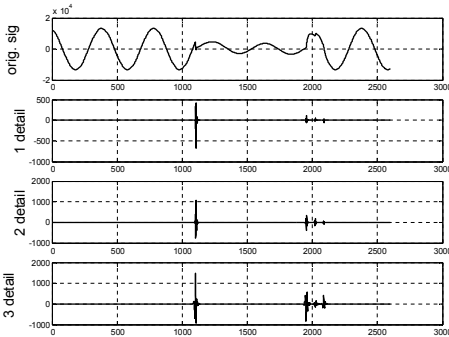


Fig. 4. Signal and its 3 details

Using a nine periods' window for the extraction of input vector for classifier it was important to find the beginning time of an event as exactly as possible. In Fig. 4 the real part of Space Phasor (Original Signal) and its detail are shown.

VI. CLASSIFICATION OF SIGNALS GIVEN BY PARAMETRIC EQUATIONS

Signal modeling by parametric equations for classifiers tests was advantageous in some aspects. It was possible to change testing and training signal parameters in wide range and in controlled manner. Signals simulated that way were very close to reality. On the other hand, different signals belonging to the same class gave the opportunity to estimate the generalization ability of classifiers based on neural networks.

Signals belonging to five main groups of disturbances [16], were simulated. The classes and respective equations are summarized in Table I. As a special group, the non-disturbed signals were chosen (pure sinusoid).

TABLE I
PARAMETRIC EQUATIONS FOR SIMULATION OF DISTURBED SIGNALS

Event	Equation
Pure Sinusoid	$v(t) = \sin(\omega t)$
Sudden Sag	$v(t) = (1 - \alpha_{ss}(1(t-t_b) - 1(t-t_e)))\sin(\omega t)$
Sudden Swell	$v(t) = (1 + \alpha_{sw}(1(t-t_1) - 1(t-t_2)))\sin(\omega t)$
Harmonics	$v(t) = \left(\begin{array}{l} \alpha_{h1} \sin(\omega t) + \alpha_{h3} \sin(3\omega t) \dots \\ + \alpha_{h5} \sin(5\omega t) + \alpha_{h7} \sin(7\omega t) \end{array} \right)$
Flicker	$v(t) = (1 + \alpha_f \sin(\beta_f \omega t))\sin(\omega t)$
Oscillatory Transient	$v(t) = \left(\begin{array}{l} (\sin(\omega t) + \alpha_{osc} \exp(-(t-t_b)/\tau_{osc})) \cdot \\ \dots \sin(\omega_{nosc}(t-t_b)) \end{array} \right)$

The ranges of signals parameter variation are shown in Table II. The variation range corresponds to values measured in real power systems.

The parameters α_{ss} and α_{sw} correspond to the depth of a sag and the measure of sudden swell respectively. The step function $1(t)$ is used to determine sag and swell duration. Flicker is characterized by its frequency $\beta_f \omega$ and amplitude α_f . Oscillatory transients are described by the frequency ω_{nosc} and the time constant of the decay τ_{osc} .

The frequency of the main component was 50 Hz and sampling rate 5 kHz. Measurement window length was 9 periods of the main component. Three-phase signals of that length were transformed into rotating space phasors and were applied to classifiers as training and test vectors.

Fig. 5 shows as an example the three-phase signal with an oscillatory transient and corresponding rotating space phasor. For a non-disturbed signal the trajectory of the space phasor is

a simple circle. The parameters of the transient are $\tau = 0.0176s$ and oscillation period $T_n = 0.0053s$ (ca. 190 Hz). Fig. 6. represents the same situation with additional 5% noise.

TABLE II
PARAMETERS VARIATION IN SIMULATED SIGNALS

Event	Parameters variation
sinus waveform	amplitude: 1, frequency: 50 Hz
sudden sag	duration: $(t_2 - t_1) = (0 - 9)T$ amplitude: $a_{ss} = 0.3 - 0.8$
sudden swell	duration: $(t_2 - t_1) = (0 - 8)T$ amplitude: $a_{sw} = 0.3 - 0.7$
harmonics	order: 3,5,7, amplitudes: 0-0.9
flicker	frequency: (5-10)Hz, amplitude: $a_f = 0.1 - 0.2$
oscillatory transient	time const.: 0.008-0.04 s frequency: 100-400Hz

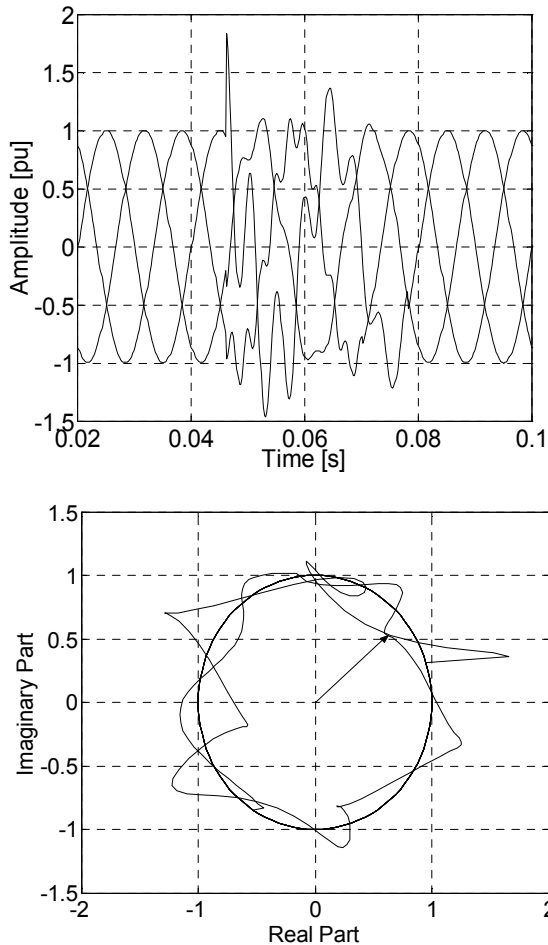


Fig. 5. Oscillatory transient; three-phase signal (above) and corresponding rotating space phasor

Higher noise levels than 5% are rather rare in electrical distribution networks.

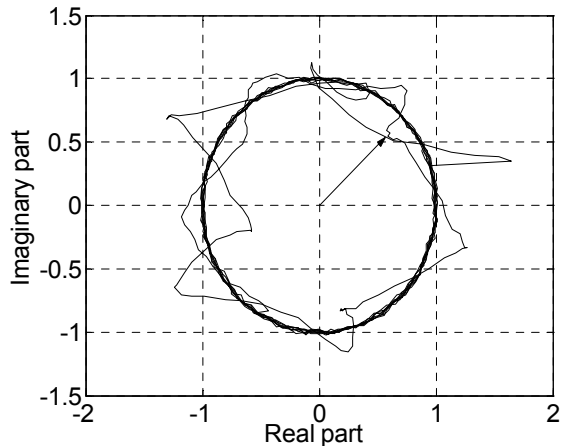
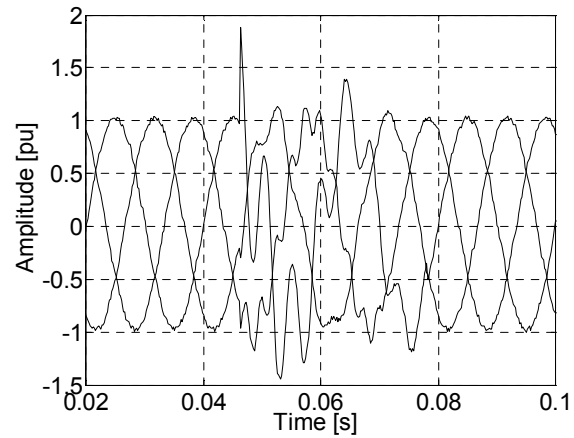


Fig. 6. Oscillatory transient; three-phase signal (above) and rotating space phasor, 5% noise

TABLE III
CLASSIFICATION RESULTS OF RBF CLASSIFIER, NO NOISE

	Sinus	Swell	Flick	Harm	Osc	Sag
Sinus	1.0	0.0	0.0	0.0	0.0	0.0
Swell	0.275	0.725	0.0	0.0	0.0	0.0
Flick	0.0	0.0	1.0	0.0	0.0	0.0
Harm	0.025	0.0	0.0	0.975	0.0	0.0
Osc	0.350	0.0	0.0	0.0	0.650	0.0
Sag	0.275	0.0	0.0	0.0	0.0	0.725

TABLE IV
CLASSIFICATION RESULTS OF SVM CLASSIFIER, NO NOISE

	Sinus	Swell	Flick	Harm	Osc	Sag
Sinus	1.0	0.0	0.0	0.0	0.0	0.0
Swell	0.025	0.975	0.0	0.0	0.0	0.0
Flick	0.0	0.0	1.0	0.0	0.0	0.0
Harm	0.025	0.0	0.0	0.975	0.0	0.0
Osc	0.0	0.0	0.0	0.0	1.0	0.0
Sag	0.025	0.0	0.0	0.0	0.0	0.975

TABLE V
CLASSIFICATION RESULTS OF RBF CLASSIFIER, 5% NOISE

	Sinus	Swell	Flick	Harm	Osc	Sag
Sinus	1.0	0.0	0.0	0.0	0.0	0.0
Swell	0.300	0.700	0.0	0.0	0.0	0.0
Flick	0.0	0.0	1.0	0.0	0.0	0.0
Harm	0.025	0.0	0.0	0.975	0.0	0.0
Oscy	0.375	0.0	0.0	0.0	0.625	0.0
Sag	0.275	0.0	0.0	0.0	0.0	0.725

TABLE VI
CLASSIFICATION RESULTS OF SVM CLASSIFIER, 5% NOISE

	Sinus	Swell	Flick	Harm	Osc	Sag
Sinus	1.0	0.0	0.0	0.0	0.0	0.0
Swell	0.025	0.975	0.0	0.0	0.0	0.0
Flick	0.0	0.0	1.0	0.0	0.0	0.0
Harm	0.025	0.0	0.0	0.975	0.0	0.0
Osc	0.0	0.0	0.0	0.0	1.0	0.0
Sag	0.025	0.0	0.0	0.0	0.0	0.975

For each of 6 classes, 50 different signals were generated, totally 300. The signals parameters were changed according to ranges given in Table II. Ten of them were used in training, other were applied in the testing phase. Parameters of the training and testing signals were changed uniformly.

Table III and Table IV illustrate the classification results obtained using RBF and SVM classifiers fed with noise free signals. Columns represent classes. Every row gives the information how many signals belonging to a class were actually correctly classified or misclassified. Numbers in cells represent classification rates given as a fraction of classified vectors to all test vectors. Presented case included 10 learning and 40 testing vectors. SVM classifier shows better classification performance, especially for oscillatory transients. By decreasing the number of training vectors the difference between RBF and SVM classifiers grows in favor of SVM.

In the presence of 5% noise in the signal the RBF classifier shows a slightly worse performance (Table V). Only one additional test vector from 40 was misclassified, by unchanged number of 10 training vectors. The SVM classifier showed the same performance with and without additive noise. The results are summarized in Table VI.

In the investigated case with 10 learning vectors, the SVM classifier shows better classification rates than RBF classifier, especially for oscillatory transients. By decreasing the number of training vectors the difference between RBF and SVM classifiers grows in favor of SVM. However, in both cases the classification rate becomes lower. Classification results obtained by SVM and RBF networks by reduced number of training vectors are summarized in Table VII and Table VIII (no noise). The number of training vectors was reduced by half in comparison to previous experiments. Using only 5 training vectors RBF network performed significantly worse especially

in the case of swells, sags and oscillatory transients.

TABLE VII
CLASSIFICATION RESULTS OF SVM CLASSIFIER, 5 TRAINING VECTORS

	Sinus	Swell	Flick	Harm	Osc	Sag
Sinus	1.0	0.0	0.0	0.0	0.0	0.0
Swell	0.022	0.978	0.0	0.0	0.0	0.0
Flick	0.044	0.0	0.956	0.0	0.0	0.0
Harm	0.022	0.0	0.0	0.978	0.0	0.0
Osc	0.422	0.0	0.0	0.0	0.578	0.0
Sag	0.022	0.0	0.0	0.0	0.0	0.978

TABLE VIII
CLASSIFICATION RESULTS OF RBF CLASSIFIER, 5 TRAINING VECTORS

	Sinus	Swell	Flick	Harm	Osc	Sag
Sinus	1.0	0.0	0.0	0.0	0.0	0.0
Swell	0.53	0.47	0.0	0.0	0.0	0.0
Flick	0.067	0.0	0.933	0.0	0.0	0.0
Harm	0.177	0.0	0.0	0.822	0.0	0.0
Osc	0.555	0.0	0.0	0.0	0.444	0.0
Sag	0.577	0.0	0.0	0.0	0.0	0.422

VII. SIMULATION AND CLASSIFICATION OF VOLTAGE SAGS

Classification of signals given by parametric equations delivered satisfactory results for a wide spectrum of disturbances. However, more detailed classification is also possible. In the first attempt, different types of voltage sags originating in power system faults were simulated and successfully classified [18]. However the influence of noise and fault resistance required further research.

Three-phase signals were generated using a model build in *Power System Blockset* [17] (Matlab) environment. The model of supply system is shown in Fig. 7. The System (SYS) is described by initial short circuit apparent power $S_k^* = 3$ GVA and voltage level of 110 kV. T1 is a two-winding (delta-ye isolated) 110/15 kV distribution transformer with $S_n = 10$ MVA. L1 and L2 are typical overhead lines with the lengths of 1.5 and 5 km respectively. Both lines supply the RL loads. The short circuit occurs at the end of the line L1.

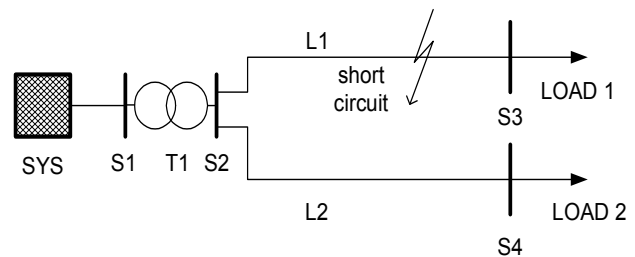


Fig. 7. Model of the supply system with one faulted line

Different fault types were simulated: three-phase and two-phase short circuits (a-b, a-c, b-c). The faults were simulated with a fault block, which allowed switching off a fault during

the zero crossing of the fault current in each phase. Faults caused voltage sags at the end of line L2.

During the investigations, 600 different cases for every fault type were simulated (totally 2400), to cover a wide range of possible configurations in real power systems. The influence of duration time of a fault and the length of the faulted line on the classification of sags were the area of interest. The short-circuited line length varied from 0.5 km to 1.5 km with the step of 200 m. For each line length and each fault type, different short-circuit times were applied. The duration of a fault varied between 0.01 s and 0.5 s. The fault clearing depended on the zero crossing of current in each phase.

Fig. 8 shows the voltage sag originating in the shortest fault time and in shortest length of line L1. Fig. 10 shows the same signal but contaminated by 5% noise.

The classifier should recognize four sag types independently from the line length and duration. The four types are sags originating in a-b-c, a-b, a-c and b-c faults. As input vectors for the classifier the voltage signals containing sags at bus S4 were used. They were transformed into space phasors. In Fig. 9 representation of the a-b sag with space phasor is shown. For every two-phase sag a 120-degree shifting of the space phasor trajectory is typical. Classification results are shown in Table IX. The noise influence on classification rate for SVM classifier was without significance. The SVM classifier was trained with only one pattern for each class, obtained for the longest fault time and shortest L1 line length, (Fig. 8, a-b-c sag, Fig. 9, a-b sag).

TABLE IX
CLASSIFICATION RESULTS OF SAGS (SVM CLASSIFIER)

	a-b-c	a-b	b-c	a-c
a-b-c	0.8542	0.0625	0.0833	0.0
a-b	0.0	1.0	0.0	0.0
b-c	0.0	0.0	1.0	0.0
a-c	0.0	0.0	0.0	1.0

The table should be interpreted as tables above. It shows good classification rates. However, for L1 line length of 1.7 km (1.2 km longer than in training) two signals were classified not correctly (those of the shortest sag duration).

TABLE X
CLASSIFICATION RESULTS OF SAGS ORDERED BY DIFFERENT FAULT RESISTANCES (SVM CLASSIFIER)

R fault	a-b-c	a-b	b-c	c-a
0.001 Ω	1.0	0.0	0.0	0.0
5 Ω	1.0	0.0	0.0	0.0
10 Ω	0.4167	0.0	0.1250	0.4583
15 Ω	0.0	0.0	0.0	1.0
...
150 Ω	0.0	0.0	0.0	1.0

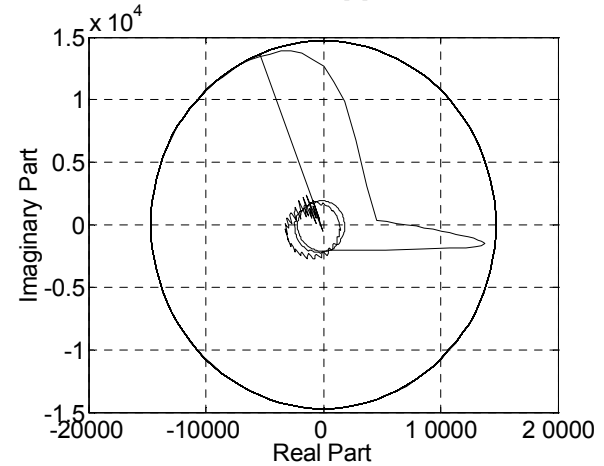
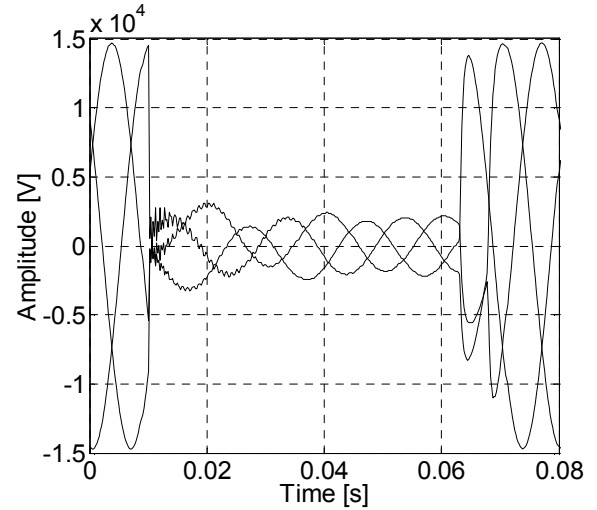


Fig. 8. Voltage three-phase sag; three-phase signal (above), rotating space phasor below.

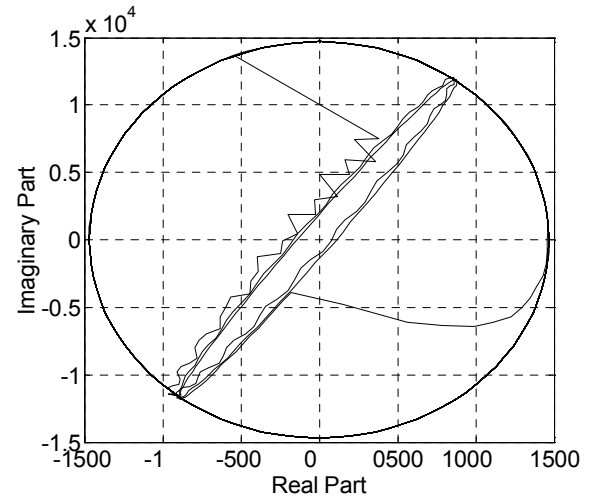


Fig. 9. Voltage two-phase sag; (a-b), rotating space phasor.

Further, decrease of L1 line length caused more misclassifications but only among a-b-c sags.

The influence of fault resistance R on the classification rate of voltage sags was also considered. Increased resistance led to smaller distinctive patterns. The classification results are summarized in Table X. It shows only misclassifications of a-b-c sags. Other types of sags were classified properly.

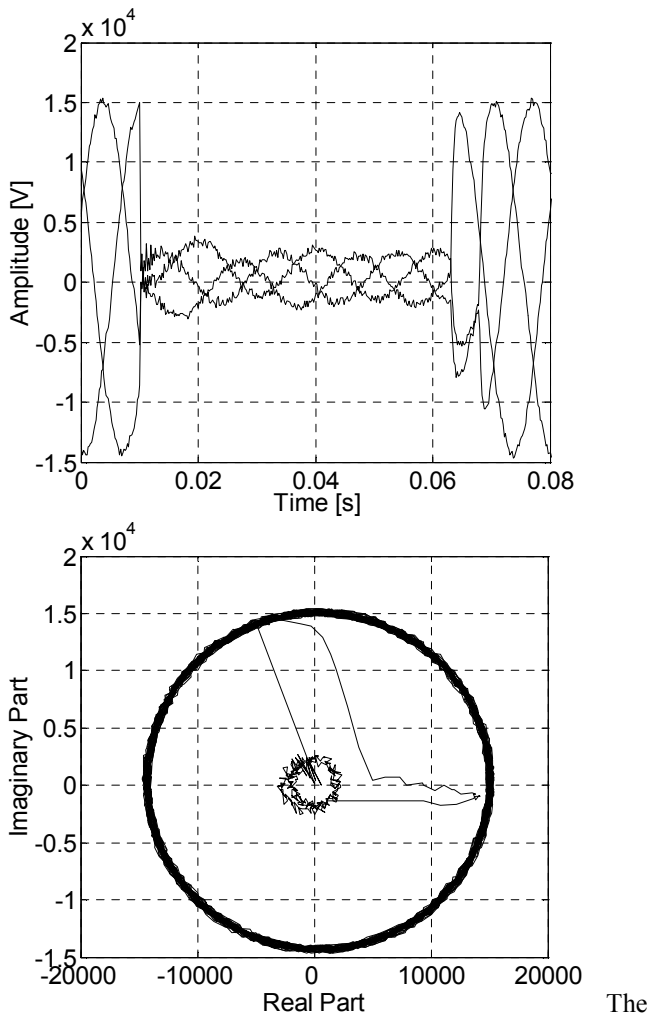


Fig 10. Voltage three-phase sag; three-phase signal (above), rotating space phasor, 5% noise

VIII. CONCLUSION

All the experiments revealed that the SVM classifier is particularly effective in the automatic classification of voltage disturbances. According to many published investigation results, the RBF neural networks are considered best tool for classification tasks. However, investigations and comparison between RBF and SVM classifiers results obtained by using parametric equations, showed better classification results for SVM networks. For this reason, the further, more in-depth investigations of the sag classifications should be carried out only for SVM classifiers. The SVM network has satisfactory generalization ability and was able to recognize sags and other disturbances correctly, for the wide range of variable parameters.

IX. REFERENCES

- [1] M. H. J. Bollen, *Understanding Power Quality Problems. Voltage Sags and Interruptions*, IEEE Press, 2000, pp. 1-4.
- [2] R. C. Dugan, M. F. McGranaghan and H. W. Beaty, *Electrical Power System Quality*, McGraw-Hill, New York, 1996, pp.1-5.
- [3] M. H. J. Bollen, "What is power quality", *Electric Power System Research*, No. 66, , pp. 5-14, July 2003

- [4] J. D. W. Patterson, *Artificial Neural Networks, Theory and Applications*, London, Prentice Hall, 1996, pp.180-213.
- [5] A. Cichocki, and R. Unbehauen, *Neural Networks for Optimization and Signal Processing*, New York, Wiley, 1993, pp.88-162
- [6] V. Vapnic, *Statistical Learning Theory*, NewYork, Springer, 1995, pp. 133-157
- [7] K. S. Chua, "Efficient computations for large least square Support Vector Machine classifiers", *Pattern Recognition Letters* 24, pp. 75-80 2003.
- [8] R. Salat and S. Osowski, "Accurate fault location in the power transmission line using support vector machine approach", *IEEE Trans. on Power Systems*, vol. 19, No. 2, May 2004, pp. 979-986.
- [9] M. Chester, *Neural Networks. A tutorial*, London, Prentice Hall, 1993, pp.50-66
- [10] Y. H. Song, Q. X. Xuan, and A. T. John, "Comparison studies of five neural networks based fault classifiers for complex transmission lines", *Electric Power System Research*, vol. 43, pp. 125-132, 1997.
- [11] W.-M Lin, C.-D. Yang, J.-H. Lin and M.-T. Tsay, "A fault classification method by RBF neural network with OLS learning procedure", *IEEE Trans. on Power Delivery*, vol. 16, No. 4, pp. 473-477, October 2001.
- [12] K. G. Narendra, V. K. Sood, K. Khorasani and R. Patel, "Application of a radial basis function (RBF) neural network for fault diagnosis in a HVDC system", *IEEE Transactions on Power Systems*, vol. 13, No. 1, February 1998, pp. 177-183.
- [13] S. Geva, J. Sitte, "Networks of Exponential Neurons for Multivariate Function Approximation", *Proc. of IJCNN Singapore*, 1991, pp.2305-2310.
- [14] T. Lobos, "Fast estimation of symmetrical components in real-time", *IEE Proc. Pt. C*, vol. 139, No. 1, pp. 85-89, Jan. 1992.
- [15] T. Lobos, J. Rezmer and H. J. Koglin, "Analysis of power system transients using wavelets and Prony method", *Proc. of 2001 IEEE Porto Power Tech Conference*, paper EMT-103.
- [16] J. Arrillaga, N. R. Watson, S. Chen, *Power System Quality Assessment*, New York, Wiley, 2000, p. 23
- [17] Power System Blockset. User's Guide, The Math Works Inc. 2000
- [18] P. Janik, T. Lobos, P. Schegner, "Classification of power quality events using SVM networks" in *Proc. 2004 Eighth IEE International Conference Developments in Power System Protection*, pp. 768-771

X. BIOGRAPHIES



Przemyslaw Janik was born in 1976 in Drawsko in Poland. After graduation from the Wrocław University of Technology in 2000 he joined Technical University in Dresden (Germany) where he worked for two years. In 2002 he joined the Faculty of Electrical Engineering at Wrocław Technical University where he works on PhD. He obtained the M. Sc. degree in 2000. His research activities are electrical power quality, neural networks and artificial intelligence classification systems.



Prof. Tadeusz Lobos received the M.Sc., Ph.D. and Habilitate Doctorate (Dr.Sc.) degrees, all in electrical engineering, from the Wrocław University of Technology, Poland, in 1960, 1967, and 1975, respectively. He has been with the Department of Electrical Engineering, Wrocław University of Technology, since 1960, where he became a Full Professor in 1989. From 1982 to 1986, he worked at the University of Erlangen-Nuremberg, Germany. His current research interests are in the areas of transients in power systems, control and protection, and especially application of neural networks and signal processing methods in power systems. The Alexander von Humboldt Foundation, Germany awarded Dr. Lobos a Research Fellowship in 1976 and he spent this fellowship at the Technical University of Darmstadt. He received the Humboldt Research Award, Germany in 1998.